Modulation of individual steps in group I intron catalysis by a peripheral metal ion

MARCELLO FORCONI,[1] JOSEPH A. PICCIRILLI,[2,3,4] and DANIEL HERSCHLAG[1]

[1]Department of Biochemistry, Stanford University, Stanford, California 94305, USA
[2]Department of Chemistry, University of Chicago, Chicago, Illinois 60637, USA
[3]Department of Biochemistry and Molecular Biology, University of Chicago, Chicago, Illinois 60637, USA
[4]Howard Hughes Medical Institute, University of Chicago, Chicago, Illinois 60637, USA

ABSTRACT

Enzymes are complex macromolecules that catalyze chemical reactions at their active sites. Important information about catalytic interactions is commonly gathered by perturbation or mutation of active site residues that directly contact substrates. However, active sites are engaged in intricate networks of interactions within the overall structure of the macromolecule, and there is a growing body of evidence about the importance of peripheral interactions in the precise structural organization of the active site. Here, we use functional studies, in conjunction with published structural information, to determine the effect of perturbation of a peripheral metal ion binding site on catalysis in a well-characterized catalytic RNA, the *Tetrahymena thermophila* group I ribozyme. We perturbed the metal ion binding site by site-specifically introducing a phosphorothioate substitution in the ribozyme's backbone, replacing the native ligands (the *pro-*R_P oxygen atoms at positions 307 and 308) with sulfur atoms. Our data reveal that these perturbations affect several reaction steps, including the chemical step, despite the absence of direct contacts of this metal ion with the atoms involved in the chemical transformation. As structural probing with hydroxyl radicals did not reveal significant change in the three-dimensional structure upon phosphorothioate substitution, the effects are likely transmitted through local, rather subtle conformational rearrangements. Addition of Cd^{2+}, a thiophilic metal ion, rescues some reaction steps but has deleterious effects on other steps. These results suggest that native interactions in the active site may have been aligned by the naturally occurring peripheral residues and interactions to optimize the overall catalytic cycle.

Keywords: enzymatic catalysis; ribozyme; peripheral interactions; metal ion; evolution

INTRODUCTION

A fundamental challenge in biochemistry is to understand how enzymes work. One of the strategies used by enzymes to achieve catalysis is the precise positioning of reactive groups within the enzyme's active site, and functional studies in a multitude of enzymes have demonstrated the importance of these active site residues in catalysis (Jencks 1987; Kraut 1988; Fersht 1999). Nevertheless, it is not just the residues traditionally considered as within the active site that are important for catalysis. For example, in carbonic anhydrase II, mutations outside the active site affect binding specificity of the catalytic metal ion inside the active site, suggesting a role for these residues in correct assembling of the catalytic core (Hunt et al. 1999). The specificity of an aminotransferase was shifted from aspartate to valine by random mutagenesis, with 16 of the 17 required substitutions outside the active site (Oue et al. 1999). Similarly, the activity of a catalytic antibody was increased 100-fold without any change in the residues directly contacting the substrate (Patten et al. 1996). Indeed, a role for mutations outside the active site in the evolution from a generalized to a specialized enzyme has been proposed on the basis of experiments on directed evolution of a bacterial phosphotriesterase, carbonic anhydrase, and serum paraoxonase (Aharoni et al. 2005; Khersonsky et al. 2006).

There are several examples of important peripheral interactions in ribozymes. For example, the structure of the HDV ribozyme active site is influenced by sequence variation outside the core (Gondert et al. 2006), and perturbation of a metal ion binding site outside of the RNase P active site has a 10^4-fold inhibitory effect on the catalytic process, probably by affecting substrate binding

Reprint requests to: Daniel Herschlag, Department of Biochemistry, Beckman Center B400, Stanford University, Stanford, CA 94305-5307, USA; e-mail: herschla@stanford.edu; fax: (650) 723-6783.

Article published online ahead of print. Article and publication date are at http://www.rnajournal.org/cgi/doi/10.1261/rna.632007.

(Christian et al. 2006). Further, a dramatic change, such as the deletion of the peripheral region P5abc in the *Tetrahymena* group I ribozyme that ablates several peripheral interactions, has a large deleterious effect on several steps of the catalytic process (Engelhardt et al. 2000), and a peripheral interaction of the hammerhead ribozyme has been shown to be central for assembly of the active site and maximal activity (Canny et al. 2004; Martick and Scott 2006).

Catalysis is generally a multistep process that involves binding events, conformational changes, as well as a chemical step, and the fine-tuning of all of the steps is important for the optimization of catalysis (Albery and Knowles 1976; Ellington and Benner 1987). Although the previous examples demonstrate the importance of peripheral interactions in RNA catalysis, they did not address the role of single peripheral interactions in the individual reaction steps and in fine-tuning of the catalytic cycle in an RNA enzyme.

To address this issue we have investigated the effect of perturbation of a single interaction in the *Tetrahymena* group I ribozyme, a well-studied ribozyme that has been extensively used as a model system to understand the basic principles of RNA catalysis (Hougland et al. 2006). We focused on interactions involving metal ions, because of the multiple and still poorly understood roles of metal ions in RNA catalysis (Feig and Uhlenbeck 1999).

Recent crystal structures of three different group I introns (Adams et al. 2004; Golden et al. 2005; Guo et al. 2005; Stahley and Strobel 2005), including a truncated version of the *Tetrahymena* ribozyme (Guo et al. 2005), show a plethora of peripheral interaction. We turned our attention to a metal ion observed in the *Azoarcus* and Twort intron crystal structures and located at the periphery of their active sites (Fig. 1A,B, M_E). To probe the presence of this peripheral metal ion in the *Tetrahymena* ribozyme, we used site-specific phosphorothioate substitutions on the RNA backbone, coupled with metal ion specificity switch experiments. Metal ion specificity switch experiments rely on the higher affinity of sulfur for Cd^{2+}, or other so-called soft metal ions, compared to Mg^{2+}, and rescue of reactivity of the sulfur-substituted ribozyme upon addition of a soft metal ion that can arise if the newly introduced sulfur atom replaces an oxygen atom that acts as a ligand for Mg^{2+} (Cohn et al. 1982; Eckstein 1983; Christian 2005; Hougland et al. 2005, 2006). To address to what extent this peripheral metal ion contributes to catalysis, we dissected the effect of perturbation of two of its binding sites on the individual reaction steps.

Our results confirm the presence of M_E in the *Tetrahymena* ribozyme. Further, we found that perturbation of two of its ligands differentially affects several reaction steps, including the chemical step. These results raise the possibility that peripheral interactions can be used by ribozymes to modulate catalysis. We speculate that the *Tetrahymena* ribozyme has optimized the interactions at this and other peripheral sites in the course of its evolution to finely tuning its catalytic cycle.

RESULTS AND DISCUSSION

A metal ion at the periphery of group I intron active site

Seven crystal structures of three group I introns are available: two structures from the *Azorcus* intron, Azo1 (Adams et al. 2004) and Azo2 (Stahley and Strobel 2005), a structure from the Twort, Two (Golden et al. 2005), and four independent molecules present in the *Tetrahymena* asymmetric cell, Tet1 to Tet4 (Guo et al. 2005). We overlaid the molecules by aligning the backbone atoms of the six conserved residues in the J8/7 region and the first two nucleotides in P7 (Fig. 1; residues 167–174, 182–189, and 301–308 in, respectively, the *Azoarcus*, Twort, and

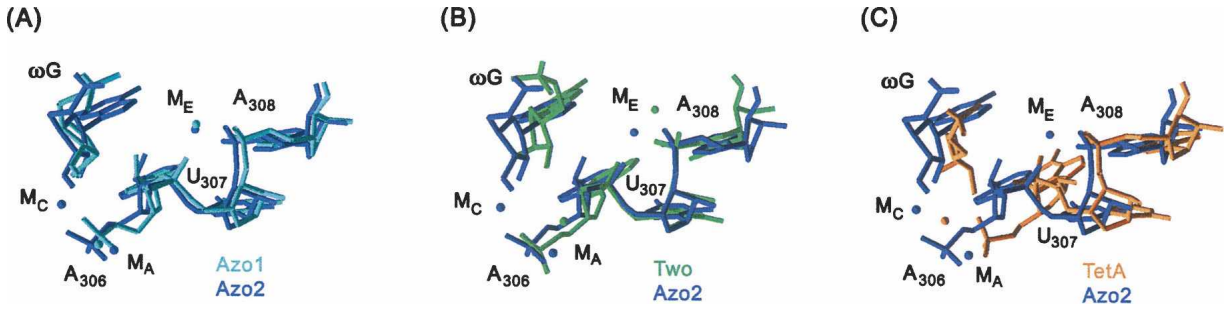

FIGURE 1. Location of M_A, M_C, and M_E in the different group I introns crystal structures. (*A*) Superposition of the first and second *Azoarcus* crystal structures (Azo1 and Azo2, respectively) (Adams et al. 2004; Stahley and Strobel 2005). (*B*) Superposition of the Twort and the second *Azoarcus* crystal structures (Two and Azo2, respectively) (Golden et al. 2005; Stahley and Strobel 2005). (*C*) Superposition of molecule A in the *Tetrahymena* and the second *Azoarcus* crystal structures (TetA and Azo2, respectively) (Guo et al. 2005; Stahley and Strobel 2005). Residues and metal ions from Azo1 are in cyan, from Azo2 in dark blue, from Two in green, and from TetA in orange. Structures were aligned using residues 301–308 (*Tetrahymena* numbering) because these residues lie in the ribozyme core and are implicated from structural and functional data as active site components.

Tetrahymena introns; henceforth, residues will be denoted using the *Tetrahymena* numbering).

Three of the crystal structures, Azo1, Azo2, and Two, show a magnesium ion outside the active site (Fig. 1; M_E), near the phosphoryl groups of residues 307 and 308. We will refer to the binding site of this metal ion as site E and to this metal ion as M_E, as there is biochemical evidence for effects from four other metal ions in or near the active site: M_A (see Fig. 2), which coordinates the 3′-oxygen of the leaving group and the *pro*-S_P oxygen of the reactive phosphoryl group (Piccirilli et al. 1993; Shan et al. 2001); M_B, which coordinates the 3′-oxygen of the guanosine nucleophile (Weinstein et al. 1997; Shan et al. 1999); M_C, which coordinates the 2′-hydroxyl of the guanosine nucleophile and the *pro*-S_P oxygen of the reactive phosphoryl group (Sjogren et al. 1997; Shan et al. 2001; Hougland et al. 2005); and M_D (not depicted in Fig. 2), which is implicated in a contact with the first adenosine of the transferred group (Shan and Herschlag 2000). Two of these metal ions (M_A and M_C) have been observed in the two *Azoarcus* crystal structures, while there is no structural evidence for M_B. This observation led to the proposal that M_B could be "recruited" in the functional tests, as discussed by Hougland et al. (2006). However, the exact number of metal ions present in the active site is not the focus of this article and is therefore not addressed further herein. We emphasize for the current work that M_E is distinct from the metal ions previously identified by biochemical tests.

TABLE 1. Distances from M_E to selected residues (indicated here using the *Tetrahymena* numbering) in *Azoarcus* (Azo1 and Azo2), Twort (Two), and *Tetrahymena* (Tet) crystal structures

	Distance (Å) from M_E to					
	U307R_P	U307S_P	A308R_P	A308S_P	A306$_{2'OH}$	N7 G414
Azo1	2.30	4.63	2.11	3.92	4.64	3.71
Azo2	2.14	4.49	1.90	3.60	3.98	3.82
Two	4.86	7.37	3.93	5.95	4.33	4.73
Tet (Azo1)	1.76	3.32	2.91	4.40	4.33	2.93
Tet (Azo2)	1.72	3.46	2.64	4.28	4.12	3.01
Tet (Two)	3.77	6.12	4.33	6.57	4.74	4.43

As M_E was not observed in the *Tetrahymena* structures, its distance from *Tetrahymena* residues was determined by superimposing each of the *Tetrahymena* structures to each of the other group I intron structures (Azo1, Azo, or Two) by fitting residues 301–308 (*Tetrahymena* numbering). The reported values are an average of the distances of each of the four molecules contained in the *Tetrahymena* asymmetric cell to M_E present in the structure indicated in parentheses.

The position of M_E is approximately the same in Azo1 and Azo2 (Fig. 1A; Table 1). This metal ion sits outside the active site, which is defined by the position of M_A and M_C and their first-sphere ligands. Putative ligands for M_E are the *pro*-R_P oxygen atoms of residues 307 and 308, which are 2.1 and 1.9 Å, respectively, from M_E in Azo2. Coordination of M_E to these two residues is consistent with the strong interference from phosphorothioate substitution observed in NAIM experiments (Strauss-Soukup and Strobel 2000). The N7 atom of the guanosine nucleophile is in the vicinity of M_E (3.8 Å), and a possible role for this atom in coordination of a metal ion in the *Tetrahymena* intron was proposed by Szostak and coworkers, based on the reduced binding affinity with 7-deazaguanosine as the nucleophile (Lin et al. 1994). Although the distance of 3.8 Å between M_E and N7 is not consistent with direct contact, a water-mediated contact is possible; alternatively, the structure observed in crystals may need to rearrange to reach the active conformation. The only other putative RNA ligand for M_E, either through an inner-sphere contact or outer-sphere coordination involving a water molecule, is the 2′-hydroxyl group of residue A306. The oxygen atom of this group is ~4 Å from M_E (Table 1), and a strong signal in NAIM experiments is consistent with an important role for this residue (Strauss-Soukup and Strobel 2000). There are no additional groups within 5 Å that can complete the coordination sphere of this metal ion; therefore, two water molecules likely serve as additional ligands. Figure 3 shows a speculative description of the complete coordination of M_E, based on the structural data and consistent with functional data.

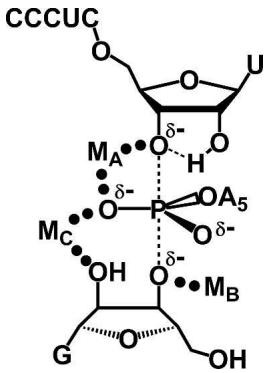

FIGURE 2. Model of the *Tetrahymena* ribozyme transition state during the first step of splicing (Shan et al. 1999, 2001; Yoshida et al. 2000).

Regardless of the precise nature of the coordination sphere of M_E, this metal ion is sufficiently distant from the atoms directly involved in the chemical transformation to rule out a direct role in the stabilization of the reaction transition state. According to a broad generalization, this metal ion may be regarded as a "structural" metal ion (Feig and Uhlenbeck 1999).

M_E is also present in the Twort structure (Two) (Golden et al. 2005). However, its position with respect to the

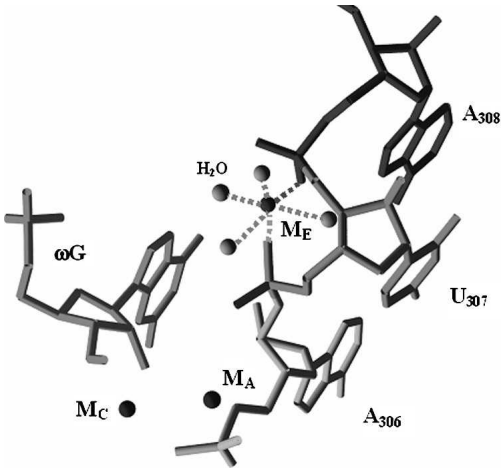

FIGURE 3. Putative M_E ligands from the second *Azoarcus* crystal structure (Stahley and Strobel 2005). Four water molecules (lighter spheres) have been modeled in the structure and were not present in the original PBD file. M_A and M_C (darker spheres) are included in the figure to help distinguish the location of the active site.

putative binding sites is different from that observed in Azo2, as shown in the overlay of the two structures (Fig. 1B; Table 1). In particular, the distance in Two from M_E to the *pro-*R_P oxygen atoms 307 and 308 is larger than in Azo2 (Table 1) and outside the range for inner-sphere contacts.

In Tet1 to Tet4, M_E was not observed. This could be due to the lack of this metal ion in the *Tetrahymena* intron; however, when Tet1 was overlaid with Azo2 (Fig. 1C), there was enough space for coordination of a metal ion to residues 307 and 308 in Tet1, as was also the case for Tet2, Tet3, and Tet4 (not shown). The average distance of M_E in the Azo2 structure to selected residues in an overlaid Tet structure is given in Table 1. It is possible that there was insufficient electron density and resolution to identify a bound Mg^{2+} at this site in the *Tetrahymena* structures. Alternatively, the lack of M_E in the *Tetrahymena* structures may arise from structural rearrangements due to the missing elements (P1, P2, P2.1, P9.1, and P9.2) in the form of this ribozyme that was crystallized (Guo et al. 2005). Nevertheless, metal ion coordination to residues 307 and 308 is consistent with NAIM data with the *Tetrahymena* intron (Strauss-Soukup and Strobel 2000), although phosphorothioate substitutions in this intron resulted in less interference compared to that for *Azoarcus*.

To determine whether M_E is present also in the *Tetrahymena* intron, and, if so, to study its effect on the individual reaction steps, we prepared two mutants, U307R_P and A308R_P, containing a single phosphorothioate substitution at positions 307 and 308, respectively (see Materials and Methods).

If M_E were important for catalysis and the *pro-*R_P phosphoryl oxygens at positions 307 and 308 were its ligands, the simplest prediction would be that the mutants bearing a phosphorothioate substitution at these positions would be less reactive than the wild-type enzyme. However, as hampered reactivity may arise for several reasons, rescue by soft metal ions such as Cd^{2+} is needed to provide strong functional evidence for a contact between a metal ion and the sulfur atom or, by analogy, the native oxygen atom (Christian 2005; Hougland et al. 2006). While artifacts due to "recruiting" a rescuing metal ion are possible, structural studies have usually provided support for metal ions identified through thio-rescue experiments (Christian 2005; Hougland et al. 2006).

We also prepared a double mutant (DM), containing both of the phosphorothioate substitutions, to investigate whether the observed effects were additive, and two control mutants, bearing the phosphorothioate substitution at the S_P position (U307S_P and A308S_P; note the longer distance from these atoms to M_E; Table 1). The *pro-*S_P oxygen at position 307 was proposed to be an outer-sphere ligand for M_A (Adams et al. 2004; Stahley and Strobel 2005), and thus the mutant ribozyme U307S_P may react slower than the wild type; however, given the proposal of indirect coordination of the substituted oxygen to a metal ion, we expected no dependence of the reactivity of this ribozyme on Cd^{2+} addition.[1]

For each mutant preparation, we also prepared a ligated wild-type ribozyme and compared its reactivity to the wild type prepared by in vitro transcription to ensure that the ligation procedure did not affect the results. When we measured the reactivity of the mutant enzymes using the oligonucleotide substrate −1d,rSA$_5$ (see Table 2), U307R_P, U307S_P, A308R_P and DM displayed a 5- to 10-fold decreases in reactivity compared to the wild-type ribozyme (WT), while A308 S_P had the same reactivity as the wild type (see Table 3). Increasing or decreasing $MgCl_2$ concentration (5–200 mM) did not change the ratio of reactivity between U307R_P and the WT ribozyme (not shown), suggesting that defects in magnesium ion occupancy are not the cause of the decrease in reactivity. Conversely, addition of 1 mM $CdCl_2$ enhanced the reactivity of U307R_P, A308R_P, and DM, bringing the reactivity of these mutants close to the wild type (see Fig. 4; Table 3), but U307S_P reactivity was not rescued (data not shown; Table 3). These data, coupled with the structural observation above, provide support for the direct coordination of a metal ion to positions 307R_P and 308R_P. In light of this finding, we next evaluated the effect of the phosphorothioate substitution on the individual reaction steps.

[1]It has been suggested that soft metal ions can rescue outer-sphere interactions in some cases, thereby complicating the analysis of metal ion rescue experiments (Basu and Strobel 1999). However, recent results indicate that the rescue previously observed arose because of uncontrolled thermodynamic differences in the behavior of P4–P6 RNA in different metal ions (J.K. Frederiksen and J.A. Piccirilli, in prep.).

TABLE 2. Rate constants, steps monitored, and 5′-splice site analog (S) used in the corresponding experiments

Measured rate constant	Step monitored	Oligonucleotide S used[a]	Abbreviation
k_3	E + S + G → P	d(CCCUC)UdA$_5$	−1r,dSA$_5$
$(k_c/K_M)_o^G$	(E•S)$_o$ + G → P	d(CCCUC)UdA$_5$	−1r,dSA$_5$
$(k_c/K_M)_c^G$	(E•S)$_c$ + G → P	CCCUCd(U)A$_5$	−1d,rSA$_5$
k_{open}	(E•S•G)$_o$ → P	CCCd(UCU)A$_5$	−(1–3)d,rSA$_5$
k_c	(E•S•G)$_c$ → P	CCCUCd(U)A$_5$	−1d,rSA$_5$
$k_{off,o}^S$	(E•S)$_o$ → E + S	CCCm(U)Cd(U)A$_5$	−3m,−1d,rSA$_5$
$k_{off,c}^S$	(E•S)$_c$ → E + S	CCCUCd(U)A$_5$	−1d,rSA$_5$
k_{on}	E•G + S → P	CCCUCUA$_5$	rSA$_5$

A full description of the conditions used is presented in Materials and Methods.
[a]Sugar residues are ribose unless otherwise stated; d = 2′-H; m = 2′-OCH$_3$.

Perturbation of a peripheral metal ion binding site affects several steps of the *Tetrahymena* ribozyme catalytic cycle

As previously stated, the *Tetrahymena* ribozyme has been extensively used as a model for RNA catalysis. Its reaction involves several steps, and a minimal framework is summarized in Scheme 1. First, the oligonucleotide substrate (S), which mimics the 5′ splice site of the normal self-splicing reaction, binds to the ribozyme, forming the so-called P1 duplex in an ''open complex,'' indicated with the ''o'' subscript in Scheme 1. The P1 duplex can then dock into the ribozyme's core, forming tertiary interactions and generating the ''closed complex,'' denoted with the ''c'' subscript in Scheme 1. Guanosine (G) can bind at any time along this framework, and there is thermodynamic coupling between guanosine binding and P1 docking (McConnell et al. 1993; Karbstein et al. 2002), resulting in increased affinity of guanosine for the closed complex relative to the open complex. When the 3′-hydroxyl of G is deprotonated and S and G are aligned in the ribozyme's active site, the reaction's chemical step can proceed, in which the deprotonated 3′-hydroxyl of guanosine attacks the phosphoryl center in a transition state stabilized by the catalytic metal ions and other interactions (Fig. 2; Hougland et al. 2006 and references therein).

We determined the kinetic and thermodynamic frameworks for the WT and the mutant ribozymes U307R_P, A308R_P, and DM as described in Materials and Methods, using the conditions reported in Table 2. To measure reactivity and binding of guanosine from the closed complex, k_c and $(K_a^G)_c$, respectively, we used the oligonucleotide substrate −1d,rSA$_5$. This substrate possesses ribose residues at the positions that make docking interactions, so that the reaction starts from the closed complex, and a single deoxyribose substitution at the cleavage site, so that the chemical step is rate limiting and the reaction is conveniently measured (Herschlag et al. 1993; Knitt and Herschlag 1996). Substitution of the 2′-hydroxyl with 2′-deoxy groups at positions −2 and −3 destabilizes the closed complex, so that the open complex becomes the stable ground state (Herschlag et al. 1993); therefore an oligonucleotide substrate with these modifications [−(1–3)d,rSA$_5$, Table 2] with saturating, excess ribozyme and guanosine was used to measure k_{open}, the single turnover reaction starting from the (E•S•G)$_o$ complex that monitors both the docking (K'_{dock}) and the chemical (k_c) steps. Similarly, $(k_c/K_M)_o^G$ was determined under the same conditions except that guanosine was subsaturating so that k_c, K_{dock}, and $(K_a^G)_c$ were monitored. $(K_a^G)_o$ was determined by following the reactivity of a substrate reacting from the open complex as a function of guanosine concentration (or of its more soluble analog, guanosine 5′-phosphate). K'_{dock} and K_{dock} were determined indirectly as described in Materials and Methods. Finally, K_a^S was determined from the ratio between the dissociation rate constant of an oligonucleotide substrate that forms stable open complex (k_{off}) and the

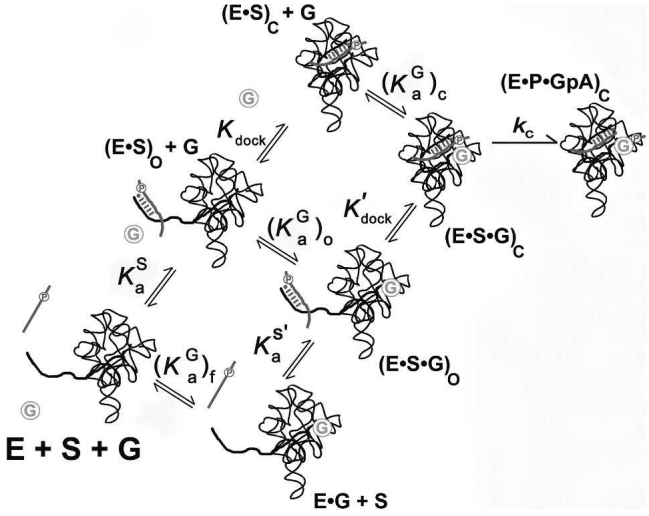

SCHEME 1.

TABLE 3. Measured values of k_c (in min^{-1}) in the absence ($^{Mg}k_c$) and presence ($^{Cd}k_c$) of 1 mM $CdCl_2$

Ribozyme	$^{Mg}k_c$	$^{Cd}k_c$	$^{Cd}k_c/^{Mg}k_c$
WT	0.040	0.040	1.0
U307R_P	0.0087	0.022	2.5
U307S_P	0.0063	0.0067	1.1
A308R_P	0.0062	0.015	2.4
A308S_P	0.033	0.030	0.91
DM	0.0082	0.024	2.9

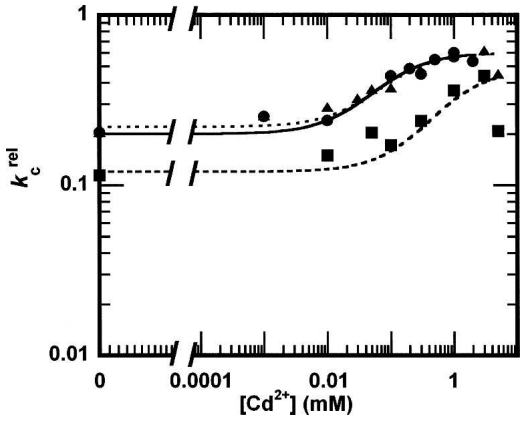

FIGURE 4. Results from one representative experiment showing rescue profiles for k_c^{rel} (defined as k_c^{mutant}/k_c^{WT}) as a function of $[Cd^{2+}]$ for U307R_P (●), A308R_P (■), and DM (▲). The Cd^{2+} concentration dependencies were fit to a single Cd^{2+} dependency: $k_{rel} = {}^{Mg}k^*\left(K_{d,app}^{Cd^{2+}} + a^*[Cd^{2+}]\right)\Big/\left([Cd^{2+}] + K_{d,app}^{Cd^{2+}}\right)$, where ${}^{Mg}k$ is the value measure in absence of $Cd^{2+}$and $a^{*Mg}k$ is the value at saturated $[Cd^{2+}]$. Values at Cd^{2+} concentrations ≥3 mM were omitted from the fit. This fit gave values of $K_{d,app}^{Cd^{2+}}$ of 0.10, 0.80, and 0.10 mM for U307R_P, A308R_P, and DM, respectively.

association constant (k_{on}) of the all-ribose substrate rSA_5, as the rate of association has been shown to be independent of the oligonucleotide used (Narlikar and Herschlag 1996).

The rate and equilibrium constants obtained for the WT ribozyme (Fig. 5A) are in agreement with those available in the literature (Herschlag and Cech 1990; Narlikar et al. 1997; Karbstein et al. 2002; Bartley et al. 2003), and the complete frameworks for the three mutant enzymes are reported in Figure 5B–D. We ensured that the chemical step was rate limiting for each of the mutants, as it is for the WT enzyme, by determining the dependence of the observed rate constant on pH (5.5–7.5) for reactions probing the "k_c step." We found no difference in the slope of the mutant enzymes compared to that of the wild type (data not shown), strongly suggesting that the chemical step was rate limiting for all of the mutants.

We quantified the effect of perturbation of M_E binding sites on the individual reaction steps of the kinetic and thermodynamic framework by calculating the differences in the mutant kinetic or thermodynamic parameters with respect to the wild-type enzyme (Fig. 6). Remarkably, each of the phosphorothioate substitutions affected several reaction steps, including five- to sevenfold effects on the chemical step. These effects occur despite the lack of direct contact between M_E and the atoms involved in bond-making and bond-breaking interactions.

The magnitude of the effects on the individual reaction steps was modest, less than 10-fold. These values are in contrast to 10^2–10^3-fold effects often observed with active site mutants in protein enzymes. However, introduction of the phosphorothioate modification is likely to weaken the affinity of the metal ion involved in the contact but not to remove it, as suggested by the lack of a differential effect on U307R_P and the wild-type ribozyme activity with varying $MgCl_2$ concentration (see above), which would provide evidence for a loss of M_E. The presence of M_E is further supported by analogous results with phosphorothioate substitutions of ligands for the catalytic metal ions, which give only small perturbations of the chemical step, suggesting that these metal ions also remain bound (Hougland et al. 2005; M. Forconi, J. Lee, and D. Herschlag, unpubl.), and that phosphorothioate substitution is not sufficient to remove the metal ions. These observations suggest that the measured effects upon perturbation of M_E binding sites represent lower limits for the overall effect of removal of M_E. In addition, small effects can be important for catalysis. For example, mutation of residues involved in substrate

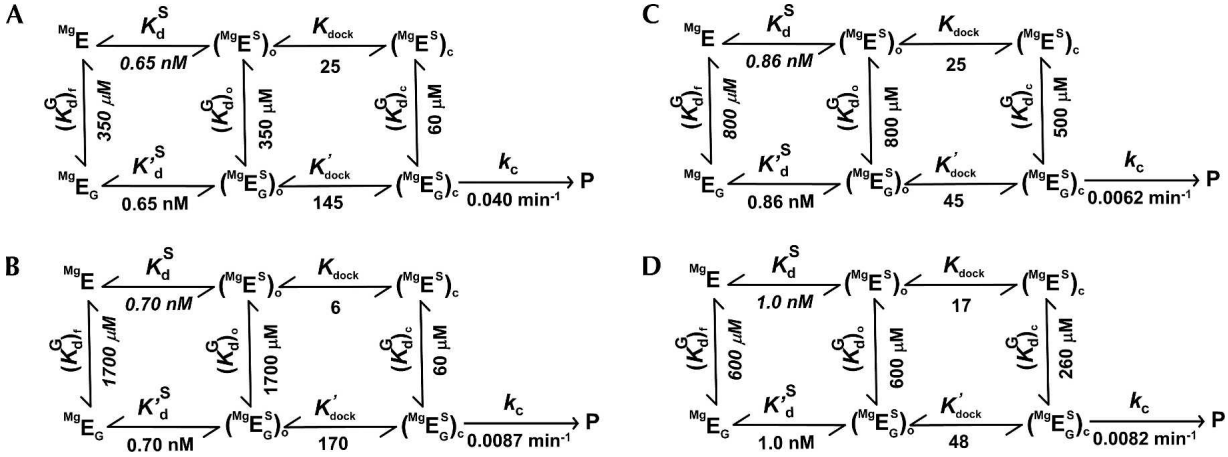

FIGURE 5. Kinetic and thermodynamic frameworks for the wild-type (*A*), U307R_P (*B*), A308R_P (*C*), and DM (*D*) ribozymes measured in 50 mM Mg^{2+}. Kinetic and thermodynamic constants were determined as described in Materials and Methods. Values of $K_d(1/K_a)$ are used instead of K_a for clarity. Values in italics are obtained from completing the thermodynamic cycles but were not directly measured.

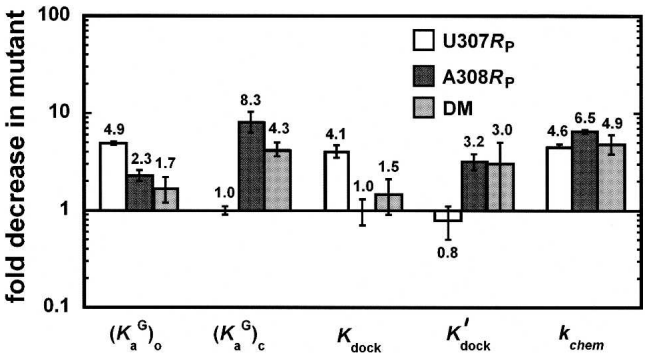

FIGURE 6. Effects of phosphorothioate substitution on the individual reaction steps for U307R_P (white bars), A308R_P (dark gray bars), and DM (light gray bars) in 50 mM Mg^{2+}. Numbers *above* or *below* the bars indicate the effect on the mutant kinetic or thermodynamic constant compared to the wild type. A value of 1.0 indicates no difference with respect to the wild type; values >1 indicate a decrease in the kinetic or thermodynamic constant in the mutant; values <1 denote an increase of the kinetic or thermodynamic constant in the mutant. Error bars represent standard deviations.

recognition in aminoacyl-tRNA synthetase (Fersht et al. 1985) and elongation factor TU (Sanderson and Uhlenbeck 2007) also gives small effects, suggesting that several interactions, each one providing a small contribution to catalysis, contribute to the fine-tuning of the overall catalytic process in these enzymes, in line with the proposals from Albery and Knowles (1976). The observed effects on several reaction steps upon perturbation of M_E binding sites raise the possibility that structural elements, peripheral to the active site, may be used to finely tune the catalytic cycle of functional RNAs. This point is elaborated below and in subsequent sections.

The ability to finely tune a catalytic cycle by changes in RNA peripheral interactions, rather than just interference with catalysis, is underscored by the observation that phosphorothioate substitutions at positions 307R_P and 308R_P gave different effects on the individual reaction steps. Phosphorothioate substitution at position 307R_P (Fig. 6, white bars) affected G binding to the open complex, $\left(K_a^G\right)_o$, and docking from the G-free ribozyme, K_{dock}, causing, respectively, a decrease of five- and fourfold relative to the WT enzyme. In contrast, the same parameters for G binding to the closed complex or docking with G already bound, $\left(K_a^G\right)_c$ and K'_{dock}, were unaffected by this phosphorothioate substitution (see Fig. 6). The greatly diminished effects subsequent to G binding or docking suggest that this substitution may misalign the free ribozyme for substrate binding, but that binding of either substrate restores the WT conformation. Nevertheless, an effect on the subsequent chemical step remains, as noted above. In contrast, A308R_P was more destabilized in the closed complex, with an eightfold decrease in $\left(K_a^G\right)_c$ and a threefold decrease in docking with G already bound (K'_{dock}) relative to the wild type ribozyme (Fig. 6, dark gray bars). These results suggest that this thio-substitution has little effect on binding of either substrate alone but that the WT coupling or communication between the substrates is essentially lost (Figs. 5, 6; Shan et al. 1999; Shan and Herschlag 2002).

We next introduced both thio-substitutions simultaneously into the ribozyme, giving the DM ribozyme. Whereas the simplest model for effects from multiple mutations predicts additive energetic effects (Wells 1990; Mildvan et al. 1992; Fersht 1999; Kraut et al. 2003), the effects were clearly not additive (i.e., not multiplicative in fold effects; see Fig. 6, light gray bars). The nonadditive effects indicate a functional interrelationship of these positions, consistent with ligation of a common metal ion and underscoring the intricate modulation of individual reaction steps by M_E and its binding site.

The observations above indicate that interactions with M_E are important for catalysis and affect multiple reaction steps. However, they do not address whether the catalytic perturbations result from global or only local or subtle structural changes. To address this question we performed hydroxyl radical footprinting mapping on the mutant ribozymes and compared the resulting profile to the profile obtained for the WT enzyme.

Hydroxyl radical footprinting suggests, at most, subtle rearrangement upon phosphorothioate substitution

Hydroxyl radical footprinting is a powerful technique to determine the solvent accessibility of the nucleic acid backbone (Tullius and Greenbaum 2005) and has been extensively used in probing the three-dimensional structure of the *Tetrahymena* ribozyme (Latham and Cech 1989; Celander and Cech 1991; Sclavi et al. 1998; Takamoto et al. 2002; Russell et al. 2006).

To establish whether the changes in reactivity upon phosphorothioate substitutions at positions 307R_P and 308R_P were due to global or local changes, we determined the hydroxyl radical footprinting profiles of U307R_P and A308R_P in the unfolded state and at 50 mM Mg^{2+} and compared them to the WT profiles obtained side by side and under the same conditions (see Materials and Methods). We did not perform the same experiments on DM, because of the larger quantities required for hydroxyl radical footprinting compared to kinetic assays. Given the similarity in the reaction parameters between this mutant and the other two, we expected this mutant to show a trend similar to the other mutants in differences or similarities to the wild type.

The overall protection pattern was the same within errors for the three enzymes (see Fig. 7A–D, reporting the raw counts observed for the three enzymes in a typical experiment) with regions in the conserved core protected relative to the unfolded ribozymes, as expected for regions buried within the globular structure or closely packed against its surface (Adams et al. 2004; Golden et al. 2005;

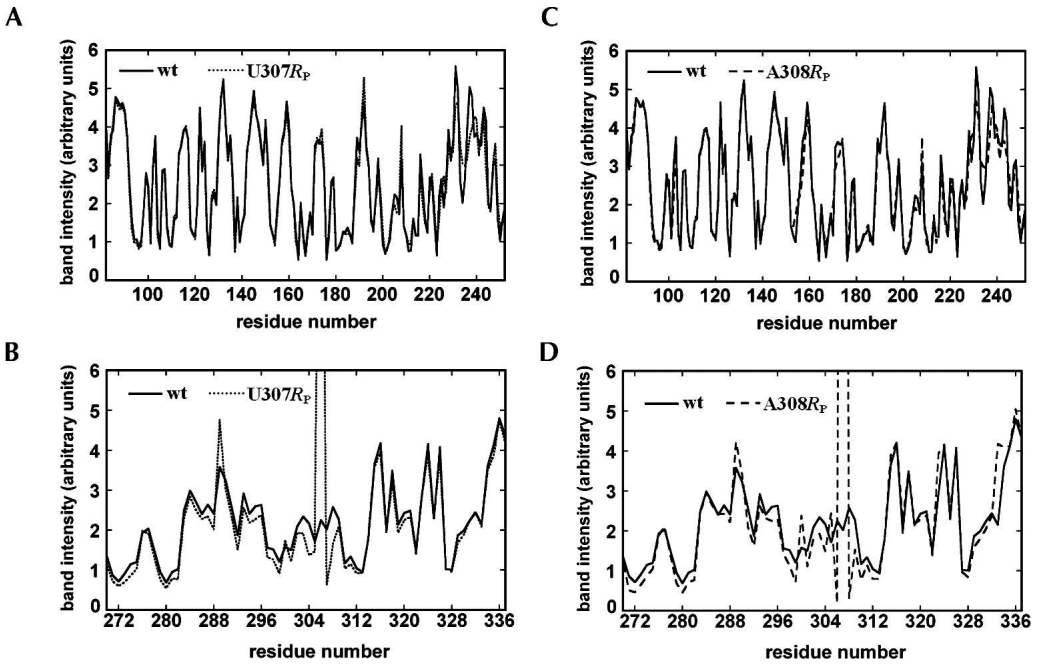

FIGURE 7. Footprinting of the wild-type (solid lines), U307R_P (dotted lines), and A308R_P (hashed lines) ribozymes in 50 mM Mg^{2+}. Representative experiment showing comparison of band intensities in hydroxyl radical footprinting for regions corresponding to (*A*) nucleotides 82–252, from 5′-radiolabeled wild-type and U307R_P ribozymes, (*B*) nucleotides 270–337, from 3′-radiolabeled wild-type and U307R_P ribozymes, (*C*) nucleotides 82–252, from 5′-radiolabeled wild-type and A308R_P ribozymes, and (*D*) nucleotides 270–337, from 3′-radiolabeled wild-type and A308R_P ribozymes.

Guo et al. 2005; Stahley and Strobel 2005). The only observable difference was at the site of phosphorothioate substitution, with mutant ribozymes displaying enhanced cleavage compared to the wild type; however, this cleavage was already present in the untreated mutant ribozymes, preventing interpretation for this position (data not shown). These results suggest that the phosphorothioate substitution introduces, at most, subtle changes in the three-dimensional structure of the mutant ribozymes and that these subtle changes can have important functional consequences.

Addition of Cd^{2+} has a complex effect on the individual reaction steps

The reactivity enhancement upon Cd^{2+} addition observed for the mutant ribozymes under k_c conditions provided a link between the introduced atomic substitution and a metal ion (Fig. 4). This proposal is in agreement with structural data, as discussed above. However, the inhibitory effect upon phosphorothioate substitution is not limited to the chemical step, but is observed in several reaction steps (Figs. 5, 6). In the simplest case of a rigidly organized structure, one might expect that interactions would or would not be formed, so that restoring an interaction would uniformly rescue all the reaction steps. Alternatively, more subtle models are possible, in which variable rearrangements can occur through the reaction cycle, and these rearrangements can be affected by local sterics and electrostatic perturbations of a bound metal ion site. As noted above, the effects upon phosphorothioate substitution provide experimental evidence for modulation through the catalytic cycle.

To further probe this modulation, we determined the effect of Cd^{2+} on the individual steps of the reaction of the three mutant enzymes. We chose to study these effects at 1 mM Cd^{2+} because inhibition occurs at higher Cd^{2+} (see Fig. 4), as is commonly observed with WT and other phosphorothioate-substituted ribozymes (Shan et al. 2001; Hougland et al. 2005). Addition of 1 mM Cd^{2+} did not give a uniform rescuing effect, as evident from Figures 8 and 9. For example, for the different mutants, the Cd^{2+} effect on G binding varied from almost complete rescue to virtually no effect, and the effect on docking ranged from no effect to inhibition.

Cd^{2+} is larger than Mg^{2+} and sulfur is larger than oxygen (see Table 4), and there are examples of local RNA structural rearrangements upon thio-substitution (Maderia et al. 2000; Smith and Nikonowicz 2000; Brannvall et al. 2001). The observed effects upon phosphorothioate substitutions and Cd^{2+} addition provide additional evidence for the ability of RNA to orchestrate subtle conformational rearrangements that have significant functional consequences and suggest that the *Tetrahymena* ribozyme may have tuned the interactions at peripheral site E to achieve optimal alignment of the groups that directly contact the substrates.

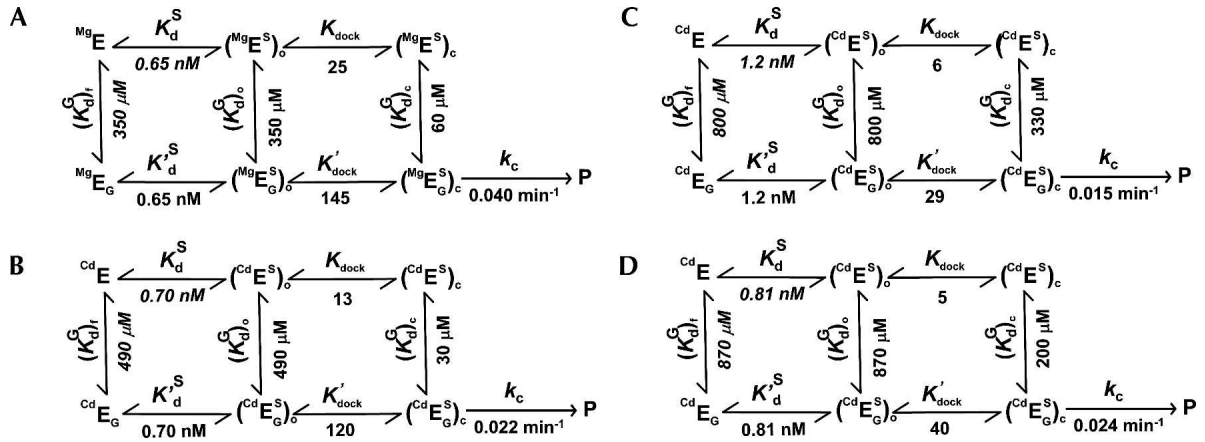

FIGURE 8. Kinetic and thermodynamic frameworks for the wild-type (*A*), U307R_P (*B*), A308R_P (*C*), and DM (*D*) ribozymes in 50 mM Mg^{2+} and 1 mM Cd^{2+}. Kinetic and thermodynamic constants were determined as explained in Materials and Methods. Values of $K_d(1/K_a)$ are used instead of K_a for clarity. Values in italics are obtained from completing the thermodynamic cycles but were not directly measured.

CONCLUSIONS

Studying enzymatic catalysis presents great challenges. One of these challenges is to unravel the connectivity that establishes active site architecture and interactions. The emergence of new crystal structures provides an opportunity to formulate hypotheses about this connectivity and to test these hypotheses using functional assays. Using the *Tetrahymena* group I ribozyme we have shown that perturbation of two binding sites of a peripheral metal ion affects several steps of the catalytic process and affects these steps differentially, highlighting an intricate catalytic connectivity that goes beyond the groups directly contacting the substrates. These observations are underscored by the differential effects upon addition of Cd^{2+} to the mutant ribozymes. This ability of metal ions to modulate different reaction steps extends their roles beyond the traditional categories of structural and catalytic.

There is an emerging literature in the protein field recognizing the importance of peripheral interactions in catalysis, specificity, and evolution (see Introduction; Hunt et al. 1999; Oue et al. 1999; Aharoni et al. 2005; Khersonsky et al. 2006). RNA enzymes can use peripheral interactions, like metal ions (Christian et al. 2006; this work), and additional helical regions (Engelhardt et al. 2000; Canny et al. 2004), to help form and align the active site. Given the sensitivity of the catalytic cycle to changes in M_E and its ligands, we suggest that the native peripheral interaction is optimal for self-splicing. It is possible that this and other peripheral interactions have played important roles in the evolution of group I introns, in line with the proposals for protein enzymes.

Given the limited repertoire of catalytic functionalities for RNA compared to proteins (Narlikar and Herschlag 1997), fine-tuning of interactions inside and outside the active site may be a particularly important strategy for ribozymes, and, again given this limited repertoire one might have imagined such fine-tuning to be more difficult for RNA enzymes. Nevertheless, such fine-tuning appears possible and may be particularly critical in orchestrating the multiple steps typical in RNA-mediated processes. It will be fascinating to understand the structural origin of the subtle effects observed in this work, to discover whether different subclasses of group I introns have used different optimization strategies in the course of their evolution, and to uncover how functional RNA/protein complexes tune interactions to carry out intricate controlled multistep processes.

MATERIALS AND METHODS

Materials

A WT in vitro transcribed *Tetrahymena* ribozyme was prepared as described previously (Zaug et al. 1988). All oligonucleotide

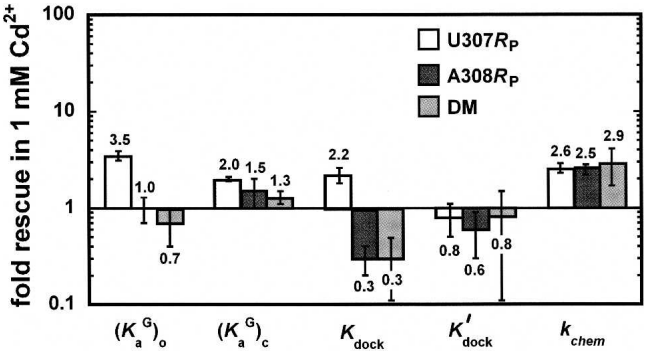

FIGURE 9. Effects of 1 mM Cd^{2+} on the individual reaction steps for U307R_P (white bars), A308R_P (dark gray bars), and DM (light gray bars). Numbers *above* or *below* the bars indicate the effect on the kinetic or thermodynamic constant in 1 mM Cd^{2+} with respect to no added Cd^{2+}. A value of 1.0 indicates no difference with Cd^{2+} added. Values <1 denote an inhibitory effect by Cd^{2+}. Values >1 indicate a stimulatory effect by Cd^{2+}. Error bars represent standard deviations.

TABLE 4. Effective ionic radii and average distances from oxygen and sulfur ligands for Mg^{2+} and Cd^{2+}

	Coordination number	Effective ionic radius[a] (Å)	M^{2+}-O[b] (Å)	M^{2+}-S (Å)
Mg^{2+}	6	0.72	2.09	2.62–2.65[c]
Cd^{2+}	6	0.95	2.30	2.50–2.70[d]

[a]Shannon (1976).
[b]Distance between metal ion and oxygen in metal ion hydrates (Ennifar et al. 2003).
[c]Distance between hexacoordinated Mg^{2+} and the sulfur atom of thiolates (Englich and Ruhlandt-Senge 2000).
[d]Distance between hexacoordinated Cd^{2+} and the sulfur atom of thiolates (Fleischer 2005).

substrates were purchased from Dharmacon Inc. and 5′-^{32}P-end-labeled using standard methods (Zaug et al. 1988). Diastereoisomers of the oligonucleotide corresponding to nucleotides 297–311 of the ribozyme, containing single phosphorothioate substitution at position U307, were separated by anion exchange HPLC (0–370 mM NaCl over 5 min, then 370–470 mM NaCl over 35 min in a background of 25 mM Tris at pH 7.4; the R_P and S_P isomers eluted at 410 and 415 mM NaCl, respectively), and desalted by Sep-Pak (Waters). Diastereoisomers of A308 and the DM were first annealed to an oligodeoxyribonucleotide of complementary sequence and then separated as hybrid duplexes by anion exchange HPLC (0–350 mM NaCl over 3 min, then 350–450 mM NaCl over 5 min and 450–600 mM NaCl over 30 min in a background of 25 mM Tris at pH 7.4). For DM, standard solid-phase synthesis yields four diasteroeisomers. We assigned the R_PR_P stereochemistry to the first oligonucleotide eluting from the column for the following reasons: (1) the R_P isomers generally elute first, and the single R_P isomers elute first from the column for both of the oligonucleotides containing the single phosphorothioate substitutions studied herein; and (2) the area corresponding to the first peak was significantly greater than that of the other peaks, in agreement with the bias toward the R_P isomeric product observed for the single mutants. The purified duplexes were precipitated by addition of three volumes of cold ethanol, resuspended in a minimal amount of water, and separated by reverse phase HPLC (0%–25% acetonitrile in 10 mM triethylammonium acetate background) at 50°C. The RNA peak was identified by comigration with one of the peaks present in the initial, unpurified RNA sample.

Ribozyme preparation

Variant ribozymes were constructed semi-synthetically using single-step three-piece ligation (Moore and Sharp 1992). Constructs corresponding to nucleotides 22–296 and 312–409 of the *Tetrahymena* ribozyme were transcribed using a DNA template produced by PCR truncation of the plasmid-encoded ribozyme sequence, with excess GMP present in the transcription of the 3′ construct (312–409) to yield a 5′ monophosphate. The 5′ construct contained a 3′-flanking hammerhead cassette to ensure homogeneous 3′ ends. The transcripts were ligated to the HPLC-purified synthetic oligonucleotides via a single-step ligation with T4 DNA ligase and a DNA splint (ATTAAGGAGAGGTCCGAC TATATCTTATGAGAAGAATACATCTTCCC) to yield a full-length ribozyme containing a single phosphorothioate mutation at the desired site. Yields were ~10% in purified, fully ligated enzyme. The ligated ribozymes were >85% active, as indicated by virtually monophasic kinetics under conditions in which oligonucleotide substrate cleavage occured faster than oligonucleotide substrate dissociation (data not shown).

General kinetic methods

All cleavage reactions were single turnover, with the ribozyme in excess of the radiolabeled 5′-splice site analog (*S), which was always present in trace quantities. Reactions were carried out at 30°C in 50 mM buffer, 50 mM $MgCl_2$, and varying concentrations of $CdCl_2$. The buffers used were NaMES (pH 5.6–6.7), NaMOPS (pH 6.5–7.7), and NaHEPES (pH 6.9–8.1). Reaction mixtures containing 10 mM $MgCl_2$ and all components except $CdCl_2$ and *S were preincubated at 50°C for 30 min to renature the ribozyme. Additional components were added and reactions were allowed to equilibrate at 30°C for 15 min before the addition of *S. Reactions were followed and analyzed as described previously (Herschlag and Cech 1990; Karbstein et al. 2002).

Determination of rate and equilibrium constants

Refer to Table 2 for definition of the measured rate and equilibrium constants and the 5′-splice site analogs (S) used in each determination. Values of k_c were determined at pH 6.9, with ribozyme saturating (20–100 nM E) with respect to S and with 2 mM G, which is essentially saturating. Values of k_{open} were determined at pH 6.9, with the ribozyme saturating (50 nM) with respect to S and with 2 mM G, and corrected for the degree of saturation using the measured values for guanosine affinity as reported in Figure 8. Values of $(k_c/K_M)_o^G$ and $(k_c/K_M)_c^G$ were determined at pH 6.9, with the ribozyme saturating (50 nM E) with respect to S and 0–50 μM G. Values of $\left(K_d^G\right)_o$ and $\left(K_d^G\right)_c$ were determined with ribozyme saturating (50 nM E) with respect to S and 0–2 mM G. Values of k_3 were determined at pH 6.9, using 0–20 nM E and 0–100 μM G.

Association constants (k_{on}) were determined at pH 6.9, 2 mM G, with varying concentration of E, using an all-ribose substrate; under these conditions, substrate binding is rate limiting (Herschlag and Cech 1990). Dissociation (k_{off}) rate constants for *S were measured by a gel mobility shift assay using pulse-chase methods (Herschlag and Cech 1990; Hougland et al. 2005). Values of K_d^S were calculated from k_{on} and k_{off} $\left(K_d^S = k_{off}/k_{on}\right)$.

K_{dock} and K'_{dock} for the WT ribozyme were taken from literature values (Bartley et al. 2003). For the mutants, K'_{dock} was determined from Equation 1, derived from the thermodynamic cycles in Figure 5, and the independently measured values of k_c^{WT} and k_c^{mutant}.

$$\frac{k_{open}^{WT}}{k_{open}^{mutant}} = \frac{K'^{WT}_{dock}}{K_{dock}^{mutant}} * \frac{k_c^{WT}}{k_c^{mutant}}. \quad (1)$$

Similarly, K_{dock} was determined from Equation 2 and the values measured in other experiments.

$$\frac{(k_{cat}/K_M)_o^{G,WT}}{(k_{cat}/K_M)_o^{G,mutant}} = \frac{K_{dock}^{WT}}{K_{dock}^{mutant}} * \frac{(K_d^G)_c^{mutant}}{(K_d^G)_c^{WT}} * \frac{k_c^{WT}}{k_c^{mutant}}. \quad (2)$$

Hydroxyl radical footprinting with Fe(II)-EDTA

The ribozyme was ^{32}P labeled at the 5′ or 3′ end using published protocols (Donis-Keller et al. 1977; Huang and Szostak 1996), purified by 8% (w/v) denaturing polyacrylamide gel electrophoresis, eluted by overnight soaking in TEN buffer (10 mM TRIS at pH 7.4, 1 mM EDTA at pH 8.0, 200 mM NaCl), and precipitated by addition of three volumes of cold ethanol and incubation at −80°C for 15 min. The ribozyme was folded as previously described, and the Mg^{2+} concentration was increased to 50 mM. The footprinting reaction was started by addition of 1.25 mM $Fe(NH_4)_2(SO_4)_2$, 1.25 mM Na-EDTA, and 100 mM sodium ascorbate to the folded or unfolded ribozyme. Reactions were allowed to proceed for 40 min at 25°C and then quenched by addition of a half volume of 30 mM thiourea. Cleavage products and a control sample cleaved by ribonuclease T1 were separated by 8% denaturing polyacrylamide (19:1 acrylamide/bisacrylamide) gel electrophoresis with different running times to resolve different regions of the RNA, imaged using a PhosphorImager, and quantified using the single-band fitting program SAFA (Das et al. 2005). Footprinting of 3′-radiolabeled ribozymes was performed five different times, to give a total of six independent measurements; footprinting of 5′-radiolabeled ribozymes was performed three different times, to give a total of seven independent measurements.

ACKNOWLEDGMENTS

We thank Rhiju Das, Alain Laederach, Jihee Lee, and members of the Herschlag and Piccirilli laboratories for helpful discussions. This work was supported by a NIH Grant GM49243 to D.H. and by a grant from the Howard Hughes Medical Institute to J.A.P. J.A.P. is an investigator at the Howard Hughes Medical Institute.

Received May 14, 2007; accepted July 13, 2007.

REFERENCES

Adams, P.L., Stahley, M.R., Kosek, A.B., Wang, J., and Strobel, S.A. 2004. Crystal structure of a self-splicing group I intron with both exons. *Nature* **430:** 45–50.

Aharoni, A., Gaidukov, L., Khersonsky, O., Gould, S.M., Roodveldt, C., and Tawfik, D.S. 2005. The ''evolvability'' of promiscuous protein functions. *Nat. Genet.* **37:** 73–76.

Albery, W.J. and Knowles, J.R. 1976. Evolution of enzyme function and the development of catalytic efficiency. *Biochemistry* **15:** 5631–5640.

Bartley, L.E., Zhuang, X., Das, R., Chu, S., and Herschlag, D. 2003. Exploration of the transition state for tertiary structure formation between an RNA helix and a large structured RNA. *J. Mol. Biol.* **328:** 1011–1026.

Basu, S. and Strobel, S.A. 1999. Thiophilic metal ion rescue of phosphorothioate interference within the *Tetrahymena* ribozyme P4–P6 domain. *RNA* **5:** 1399–1407.

Brannvall, M., Mikkelsen, N.E., and Kirsebom, L.A. 2001. Monitoring the structure of *Escherichia coli* RNase P RNA in the presence of various divalent metal ions. *Nucleic Acids Res.* **29:** 1426–1432. doi: doi: 10.1093/nar/29.7.1426.

Canny, M.D., Jucker, F.M., Kellogg, E., Khvorova, A., Jayasena, S.D., and Pardi, A. 2004. Fast cleavage kinetics of a natural hammerhead ribozyme. *J. Am. Chem. Soc.* **126:** 10848–10849.

Celander, D.W. and Cech, T.R. 1991. Visualizing the higher-order folding of a catalytic RNA molecule. *Science* **251:** 401–407.

Christian, E.L. 2005. Identification and characterization of metal ion binding by thiophilic metal ion rescue. In *Handbook of RNA biochemistry* (ed. R.K. Hartmann), pp. 319–344. Wiley-VCH, Weinheim, Germany.

Christian, E.L., Smith, K.M.J., Perera, N., and Harris, M.E. 2006. The P4 metal binding site in RNase P RNA affects active site metal affinity through substrate positioning. *RNA* **12:** 1463–1467.

Cohn, M., Shih, N., and Nick, J. 1982. Reactivity and metal-dependent stereospecificity of the phosphorothioate analogs of ATP in the arginine kinase reaction. Structure of the metal-nucleoside triphosphate substrate. *J. Biol. Chem.* **257:** 7646–7649.

Das, R., Laederach, A., Pearlman, S.M., Herschlag, D., and Altman, R.B. 2005. SAFA: Semi-automated footprinting analysis software for high-throughput identification of nucleic acid footprinting experiments. *RNA* **11:** 344–354.

Donis-Keller, H., Maxam, A.M., and Gilbert, W. 1977. Mapping adenines, guanines, and pyrimidines in RNA. *Nucleic Acids Res.* **4:** 2527–2538. doi: 10.1093/nar/4.8.2527.

Eckstein, F. 1983. Phosphorothioate analogs of nucleotides—Tools for the investigation of biochemical processes. *Angew. Chem. Int. Ed. Engl.* **22:** 423–439.

Ellington, A.D. and Benner, S.A. 1987. Free energy differences between enzyme bound states. *J. Theor. Biol.* **127:** 491–506.

Engelhardt, M.A., Doherty, E.A., Knitt, D.S., Doudna, J.A., and Herschlag, D. 2000. The P5abc peripheral element facilitates preorganization of the *Tetrahymena* Group I ribozyme for catalysis. *Biochemistry* **39:** 2639–2651.

Englich, U. and Ruhlandt-Senge, K. 2000. Thiolates, selenolates, and tellurolates of the *s*-block elements. *Coord. Chem. Rev.* **210:** 135–179.

Ennifar, E., Walter, P., and Dumas, P. 2003. A crystallographic study of the binding of 13 metal ions to two related RNA duplexes. *Nucleic Acids Res.* **31:** 2671–2682. doi: 10.1093/nar/gkg350.

Feig, A.L. and Uhlenbeck, O.C. 1999. The role of metal ions in RNA biochemistry. In *The RNA world* (eds. R.F. Gesteland et al.), pp. 287–319. Cold Spring Harbor Laboratory Press, Cold Spring Harbor, New York.

Fersht, A.R. 1999. *Structure and mechanism in protein science*. W.H. Freeman and Company, New York.

Fersht, A.R., Shi, J., Knill-Jone, J., Lowe, D.M., Wilkinson, A.J., Blow, D.M., Brick, P., Carter, P., Waye, M.M.Y., and Winter, G. 1985. Hydrogen bonding and biological specificty analysed by protein engineering. *Nature* **314:** 235–238.

Fleischer, H. 2005. Structural chemistry of complexes of $(n-1)d^{10}$ ns^{m} metal ions with β-N-donor substituted thiolate ligands (m = 0,2). *Coord. Chem. Rev.* **249:** 799–827.

Golden, B.L., Kim, H., and Chase, E. 2005. Crystal structure of a phage Twort Group I ribozyme-product complex. *Nat. Struct. Mol. Biol.* **12:** 82–89.

Gondert, M.E., Tinsley, R.A., Rueda, D., and Walter, N.G. 2006. Catalytic core structure of the *trans*-acting HDV ribozyme is subtly influenced by sequence variation outside the core. *Biochemistry* **45:** 7563–7573.

Guo, F., Gooding, A.R., and Cech, T.R. 2005. Structure of the *Tetrahymena* ribozyme: Base triple sandwich and metal ion at the active site. *Mol. Cell* **16:** 351–362.

Herschlag, D. and Cech, T.R. 1990. Catalysis of RNA cleavage by the *Tetrahymena thermophila* ribozyme. 1. Kinetic description of the reaction of an RNA substrate complementary to the active site. *Biochemistry* **29:** 10159–10171.

Herschlag, D., Eckstein, F., and Cech, T.R. 1993. Contributions of 2′-hydroxyl groups of the RNA substrate to binding and catalysis by the *Tetrahymena* ribozyme. An energetic picture of an active site composed of RNA. *Biochemistry* **32:** 8299–8311.

Hougland, J.L., Kravchuk, A.V., Herschlag, D., and Piccirilli, J.A. 2005. Functional identification of catalytic metal ion binding sites within RNA. *PLoS Biol.* **3:** 1536–1548. doi: 10.1371/journal.pbio.0030277.

Hougland, J.L., Piccirilli, J.A., Forconi, M., Lee, J., and Herschlag, D. 2006. How the group I intron works: A case study of RNA

structure and function. In *The RNA world* (eds. R.F. Gesteland et al.), pp. 133–206. Cold Spring Harbor Laboratory Press, Cold Spring Harbor, New York.
Huang, Z. and Szostak, J. 1996. A simple method for 3′-labeling of RNA. *Nucleic Acids Res.* **24:** 4360–4361. doi: 10.1093/nar/24.21.4360.
Hunt, J.A., Ahmed, M., and Fierke, C.A. 1999. Metal binding specificity in carbonic anhydrase is influenced by conserved hydrophobic core residues. *Biochemistry* **38:** 9054–9062.
Jencks, W.P. 1987. *Catalysis in chemistry and enzymology*. Dover, New York.
Karbstein, K., Carroll, K.S., and Herschlag, D. 2002. Probing the *Tetrahymena* group I ribozyme reaction in both directions. *Biochemistry* **41:** 11171–11183.
Khersonsky, O., Roodveldt, C., and Tawfik, D.S. 2006. Enzyme promiscuity: Evolutionary and mechanistic aspects. *Curr. Opin. Chem. Biol.* **10:** 498–508.
Knitt, D.S. and Herschlag, D. 1996. pH dependencies of the *Tetrahymena* ribozyme reveal an unconventional origin of an apparent pK_a. *Biochemistry* **35:** 1560–1570.
Kraut, J. 1988. How do enzymes work? *Science* **242:** 533–540.
Kraut, D.A., Carroll, K.S., and Herschlag, D. 2003. Challenges in enzyme mechanism and energetics. *Annu. Rev. Biochem.* **72:** 517–571.
Latham, J.A. and Cech, T.R. 1989. Defining the inside and outside of a catalytic RNA molecule. *Science* **245:** 276–282.
Lin, C.W., Hanna, M., and Szostak, J.W. 1994. Evidence that the guanosine substrate of the *Tetrahymena* ribozyme is bound in the anti conformation and that N7 contributes to binding. *Biochemistry* **33:** 2703–2707.
Maderia, M., Horton, T.E., and DeRose, V.J. 2000. Metal interactions with a GAAA RNA tetraloop characterized by 31P NMR and phosphorothioate substitutions. *Biochemistry* **39:** 8193–8200.
Martick, M. and Scott, W.G. 2006. Tertiary contacts distant from the active site prime a ribozyme for catalysis. *Cell* **126:** 309–320.
McConnell, T.S., Cech, T.R., and Herschlag, D. 1993. Guanosine binding to the *Tetrahymena* ribozyme: Thermodynamic coupling with oligonucleotide binding. *Proc. Natl. Acad. Sci.* **90:** 8362–8366.
Mildvan, A.S., Weber, D.J., and Kuliopulos, A. 1992. Quantitative interpretations of double mutations of enzymes. *Arch. Biochem. Biophys.* **294:** 327–340.
Moore, M.J. and Sharp, P.A. 1992. Site-specific modification of pre-mRNA—The 2′-hydroxyl groups at the splice sites. *Science* **256:** 992–997.
Narlikar, G. and Herschlag, D. 1996. Isolation of a local tertiary folding transition in the context of a globally folded RNA. *Nat. Struct. Mol. Biol.* **3:** 701–710.
Narlikar, G.J. and Herschlag, D. 1997. Mechanistic aspects of enzymatic catalysis: Lessons from comparison of RNA and protein enzymes. *Annu. Rev. Biochem.* **66:** 19–59.
Narlikar, G.J., Koshla, M., Usman, N., and Herschlag, D. 1997. Quantitating tertiary binding energies of 2′-OH groups on the P1 duplex of the *Tetrahymena* ribozyme: Intrinsic binding energy in an RNA enzyme. *Biochemistry* **36:** 2465–2477.
Oue, S., Okamoto, A., Yano, T., and Kagamiyama, H. 1999. Redesigning the substrate specificity of an enzyme by cumulative effects of the mutations of non-active site residues. *J. Biol. Chem.* **274:** 2344–2349.
Patten, P.A., Gray, N.S., Yang, P.L., Marks, C.B., Wedemayer, G.J., Boniface, J.J., Stevens, R.C., and Schultz, P.G. 1996. The immunological evolution of catalysis. *Science* **271:** 1086–1091.
Piccirilli, J.A., Vyle, J.S., Cartuhers, M.H., and Cech, T.R. 1993. Metal-ion catalysis in the *Tetrahymena* ribozyme reaction. *Nature* **361:** 85–88.
Russell, R., Das, R., Suh, H., Travers, K.J., Laederach, A., Engelhardt, M.A., and Herschlag, D. 2006. The paradoxical behavior of a highly structured misfolded intermediate in RNA folding. *J. Mol. Biol.* **363:** 531–544.
Sanderson, L.E. and Uhlenbeck, O.C. 2007. Directed mutagenesis reveals amino acid residues involved in elongation factor Tu binding to yeast Phe-tRNAPhe. *J. Mol. Biol.* **368:** 119–130.
Sclavi, B., Sullivan, M., Chance, M.R., Brenowitz, M., and Woodson, S.A. 1998. RNA folding at millisecond intervals by synchrotron hydroxyl radical footprinting. *Science* **279:** 1940–1943.
Shan, S. and Herschlag, D. 2000. An unconventional origin of metal-ion rescue and inhibition in the *Tetrahymena* group I ribozyme reaction. *RNA* **6:** 795–813.
Shan, S. and Herschlag, D. 2002. Dissection of a metal-ion-mediated conformational change in the *Tetrahymena* ribozyme catalysis. *RNA* **8:** 861–872.
Shan, S., Yoshida, A., Piccirilli, J.A., and Herschlag, D. 1999. Three metal ions at the active site of the *Tetrahymena* group I ribozyme. *Proc. Natl. Acad. Sci.* **96:** 12299–12304.
Shan, S., Kravchuk, A.V., Piccirilli, J.A., and Herschlag, D. 2001. Defining the catalytic metal ions interactions in the *Tetrahymena* ribozyme reaction. *Biochemistry* **40:** 5161–5171.
Shannon, R.D. 1976. Revised effective ionic radii and systematic studies of interatomic distances in halides and chalcogenides. *Acta Crystallogr. A* **32:** 751–767.
Sjogren, A.J., Petterson, E., Sjoberg, B.M., and Stromberg, R. 1997. Metal ion interaction with cosubstrate in self-splicing group I introns. *Nucleic Acids Res.* **25:** 648–653.
Smith, J.S. and Nikonowicz, E.P. 2000. Phosphorothioate substitution can substantially alter RNA conformation. *Biochemistry* **39:** 5642–5652.
Stahley, M.R. and Strobel, S.A. 2005. Structural evidence for a two-metal-ion mechanism of group I intron splicing. *Science* **309:** 1587–1590.
Strauss-Soukup, J.K. and Strobel, S.A. 2000. A chemical phylogeny of group I Introns based upon interference mapping of a bacterial ribozyme. *J. Mol. Biol.* **302:** 339–358.
Takamoto, K., He, Q., Morris, S., Chance, M.R., and Brenowitz, M. 2002. Monovalent cations mediated formation of native tertiary structure of the *Tetrahymena termophila* ribozyme. *Nat. Struct. Mol. Biol.* **9:** 928–933.
Tullius, T.D. and Greenbaum, J.A. 2005. Mapping nucleic acid structure by hydroxyl radical cleavage. *Curr. Opin. Chem. Biol.* **9:** 127–134.
Weinstein, L.B., Jones, B., Cosstick, R., and Cech, T.R. 1997. A second catalytic metal ion in a group I ribozyme. *Nature* **388:** 805–808.
Wells, J.A. 1990. Additivity of mutational effects in proteins. *Biochemistry* **29:** 8509–8517.
Yoshida, A., Shan, S., Herschlag, D., and Piccirilli, J.A. 2000. The role of the cleavage site 2′-hydroxyl in the *Tetrahymena* group I ribozyme reaction. *Chem. Biol.* **7:** 85–96.
Zaug, A.J., Grosshans, C.A., and Cech, T.R. 1988. Sequence-specific endoribonuclease activity of the *Tetrahymena* ribozyme-enhanced cleavage of certain oligonucleotide substrates that form mismatched ribozyme substrate complexes. *Biochemistry* **27:** 8924–8931.